

# Enabling Lightweight, High Load Aero-Bearings

J.C. Avelar-Batista Wilson <sup>a\*</sup>, S. Banfield <sup>a</sup>, G. Cassar <sup>b</sup>, A. Leyland <sup>b</sup>, A. Matthews <sup>b</sup>, P. Smith <sup>c</sup>,  
B. Karadia <sup>d</sup>, N. Vaghela <sup>d</sup>, J. Housden <sup>a</sup>

<sup>a</sup> Tecvac Ltd, Buckingham Business Park, Swavesey, Cambridge, CB24 4UG, UK

<sup>b</sup> The University of Sheffield, Department of Engineering Materials, Sir Robert Hadfield Building, Portobello Street, Sheffield, S1 3JD, UK

<sup>c</sup> NMB-Minebea UK Ltd, Doddington Road, Lincoln, LN2 3QU, UK

<sup>d</sup> Airbus UK, Filton, Bristol, BS99 7AR, UK

## \* Corresponding author:

Dr J.C. Avelar-Batista Wilson

Tecvac Ltd

Buckingham Business Park, Rowles Way

Swavesey, Cambridge

CB24 4UG

UNITED KINGDOM

Phone: + 44 1954 233700 (switchboard); + 44 1954 233715

Fax: + 44 1954 233733

Email: [junia.avelar-batista@tecvac.com](mailto:junia.avelar-batista@tecvac.com)

**Keywords:** Titanium alloy, High load aero-bearings, Plasma diffusion treatments, PVD coatings

## Abstract

Environmental and commercial considerations are strongly driving research into weight saving in aircraft. In this research, innovative manufacturing processes were developed to produce lightweight titanium alloy bearings capable of withstanding high bearing pressures. This will enable the replacement of heavier conventional bearing materials with titanium alloy bearings of the same size thereby saving weight. Plasma processing and PVD coating techniques were refined and combined and a sound scientific understanding of the resulting novel processes developed to assure high performance, reliability and repeatability. These techniques were applied to test discs and small bearing (bush) samples, which were tested under progressively greater loads (pressures). FEA was also used to evaluate pressure distribution in a bush test assembly. The novel treatment has potential applications for many bearings and bearing surfaces throughout aircraft.

## 1. Introduction

Metal-to-metal spherical bearings have been widely used in the aerospace industry. Conventionally, stainless steel and copper alloy have been used respectively as materials for the inner and outer races in landing gear bearings [1]. These materials do not gall in areas where no lubricant is present but are relatively heavy. Replacement of these conventional materials by lightweight titanium alloys would enable significant weight savings, reduce fuel consumption and decrease environmental pollution. However, titanium alloy is too soft for metal-to-metal contact and tends to gall very quickly under load.

Significant improvements in the tribological properties of titanium and its alloys have been reported when these materials were subjected to surface hardening (diffusion) treatments, including nitriding [2-5] and oxidation [6-9]. Metal-to-metal aircraft bearings must be wear, corrosion and fatigue resistant. However, surface hardening treatments performed at temperatures higher than 700°C usually promote a considerable reduction in the fatigue life of the parent Ti6Al4V alloy, impairing its usage in aircraft bearings. In order to avoid galling of titanium alloys in aircraft bearing applications, triode plasma treatments (e.g., nitriding and/or oxidation) followed by PVD coatings seem to have potential, as hardened graded surfaces are produced with improved tribological properties. For instance, triode plasma nitriding treatments previously carried out in Ti6Al4V alloy at 700°C for 4 hours yielded 30-40 µm thick nitrided layers [10].

Ti6Al4V landing gear bearings treated with Nitron (triode plasma nitriding followed by PVD TiN coating) were able to withstand 80 MPa pressures without failing [1]. However, there is scope to further extend the bearing-pressure-limitation of lightweight titanium alloys without impairing the fatigue life. Pressures of 220 MPa are typical maximum pressures predicted for bearings in modern aircraft design. Achieving the 220 MPa pressure will enable the use of lightweight alloys in a large range of excessive-load-bearing applications.

In this paper, a range of triode plasma treatments (nitriding and oxynitriding) followed by PVD coatings (TiN and CrAlN) is presented. The potential of these treatments for metal-to-metal bearings is shown through bush tests carried out at progressively increasing loads. Finite element analysis (FEA) of contact pressures on bushes is also presented. Bush test results are also corroborated by reciprocating wear results that show how these treatments can improve wear/galling behaviour of untreated Ti6Al4V alloys.

## 2. Experimental

### 2.1. Triode plasma treatments (TPT) and PVD coatings

Triode plasma nitriding (TPN) and triode plasma oxynitriding (TPON) treatments were carried out in a Tecvac IP70 PVD machine. Polished Ti6Al4V test discs in annealed condition, 30 mm in diameter and 3 mm thick (350 HV<sub>0.05</sub>,  $R_a = 0.04 \pm 0.01$  µm) were treated along with Ti6Al4V inner and outer bushes (Fig.1) in annealed condition, having a surface finish of  $R_a = 0.3-0.4$  µm, which is typically found in the actual metal-to-metal aircraft bearings.

All triode plasma treatments (TPT) were performed at 700°C. Before TPT processing, test discs and bushes were subjected to a sputter clean stage using argon. Process conditions of all TPT treatments investigated are illustrated in Table 1.

Tecvac commercial TiN and CrAlN coatings were deposited onto untreated (i.e., without TPT) and TPT-treated test discs and bushes using electron beam PVD below 500°C.

Treatment hardness and depth was evaluated using Knoop microhardness measurements on polished cross-sections under a load of 0.245 N (25 gf). Martens hardness was measured using a Fischer Hardness Tester HM2000 XYP equipped with a Vickers indenter under final loads of 10 and 750 mN at the sample surface. A final load of 2mN was also used in selected TPT

samples (i.e., without coating). Coating thickness was evaluated using ball cratering. Surface roughness was also measured on untreated and TPT-treated test discs to assess how TPT and/or PVD coating processes altered the initial surface finish.

Glancing angle X-ray diffraction (GAXRD) analyses were carried out to identify near-surface phases which resulted from TPT treatments. GAXRD measurements were performed with a Siemens D5000 diffractometer with a Cu  $K\alpha$  radiation ( $\lambda=0.154056$  nm, tube voltage = 40 kV, current = 30 mA). The diffractograms were recorded with a  $2\theta$  step of  $0.02^\circ$  from  $30^\circ$  to  $60^\circ$ , step time of 5 seconds and incidence angle of  $2^\circ$ .

Scratch tests were carried out in PVD-coated and duplex (i.e., TPT followed by PVD coating) samples to evaluate coating/substrate adhesion. The radius of the diamond indenter was 0.2 mm and the measurements were performed at an increasing load rate of  $10 \text{ N mm}^{-1}$ . The sample surface and diamond tip were cleaned with isopropanol (IPA) before each scratch. For all samples, three critical loads were recorded from a set of three scratches on each specimen:  $L_{C1}$  was taken as the load at which cohesive failures (e.g. cracking, chipping of the coating) occurred;  $L_{C2}$  was the load corresponding to first occurrence of adhesive failure (i.e, the load at which the substrate was first exposed); and  $L_{C3}$  was the load at which the PVD coating was completely removed from the scratch channel.

## 2.2. Bush tests

Bush tests have been used to screen the different TPT and/or PVD coating treatments. The bush tests were used to determine the maximum pressure that surface treatments would survive. This maximum pressure could then be extrapolated to the pressures found on metal-to-metal landing gear bearings. During the test, a load is applied onto the cylindrical bush assembly through a load plate and the resulting torque and displacement wear/movement are monitored as a function of test cycles. The bush assembly comprises an inner bush which is slid into an outer bush. The inner bush is attached to a shaft that rotates  $\pm 1.5^\circ$  along its axis under the applied test load (see Fig.1) and the outer bush is fixed to the load plate. A test cycle is defined as the time for a full shaft displacement of  $\pm 1.5^\circ$  ( $6.0^\circ$  total swept angle) along its axis.

When a given treatment fails, a rapid increase in torque is registered along with significant displacement wear. TPT and/or PVD coating systems were given either a PASS or FAIL result in bush tests. The PASS mark was given to bushes that withstood a certain test load up to 6,000 cycles without failing, i.e., no rapid increase in torque or significant displacement wear. Bush tests were carried out at progressively increasing test loads. Before the start of each test the bush assembly was greased with Aeroshell 33 at the inner bush/outer bush interface. After the test, all inner and outer bush pairs were inspected and coating detachment was clearly seen in all those bush samples that were given a FAIL result. Conversely, PVD coating and TPT layers that were intact in the bush samples were given a PASS result.

## 2.3. Finite Element Analysis (FEA) of bush tests

A non-linear contact finite element analysis on the test bush assembly was performed to determine the stress distribution on the contacting surfaces of a cylindrical bush assembly with a defined clearance under an applied vertical load of 50 kN. The major objective was to evaluate the magnitude of the contacting stresses at the interface of the inner and outer bushes. A Ti6Al4V bush assembly was modelled with a nominal radial clearance of 0.025mm. The finite element model consisted of 4 parts: inner bush, outer bush, load plate and shaft (Fig.1). The shaft length was equal to the bush width (20.0 mm), whilst the outside diameter was modelled at 19.000 mm giving a radial clearance of 0.0375 mm. The load plate was modelled as a nominal 100 mm square with a hole at the centre resulting in a radial clearance of 0.025 mm relative to the outside diameter of the outer bush.

A CosmosM GeoStar V2.95 (29522 - 2005/250) software was used to perform non-linear finite element analyses. The full assembly was modelled with 8 node solid brick elements with surface to node contact defined at three interfaces labelled 1, 2 and 3 (Fig.1). The number of nodal points and elements used in the model were 20,413 and 18,944 respectively. Truss elements were added to the model for stability of the Young's modulus. A test load of 50 kN along the y-axis was used in the model. Boundary conditions included a displacement in the y-axis to the bottom surface of the load plate to simulate the test load (Fig.1) and additional displacement constraints ( $u_x = 0$ ) were added to four identical edge curves to prevent solid body rotation of the plate at loads above 80kN. The lower half of the shaft was grounded to both faces of the inner bush and a displacement constraint equal to  $u_z = 0$  was added.

#### *2.4. Reciprocating sliding wear tests on Ti6Al4V discs*

Reciprocating sliding wear tests were performed on PVD-coated and TPT-treated + PVD-coated Ti6Al4V test discs (Table 2) to the ASTM G133-95 standard under unlubricated conditions. A frequency of 4 Hz, speed of  $0.1 \text{ m s}^{-1}$  and a stroke length of 10 mm were used throughout. Specimens were cleaned in acetone and then rinsed in isopropanol before each test. Two test loads have been used: 4.0 N and 13.5 N, corresponding to initial contact pressures of approximately 0.7 and 1.0 GPa, respectively. WC-Co and sapphire balls, both 10 mm in diameter, were used to test Ti6Al4V discs coated with TiN and CrAlN, respectively. WC-Co was found to suffer significant wear when run against CrAlN-coated/treated discs at the higher load. In order to minimise changes in contact pressure during the test, sapphire balls were therefore used for CrAlN-coated/treated samples. Several tests were performed at a pre-set sliding distance and the average volume loss was recorded for each pre-set sliding distance, which was progressively increased until a significant volume loss was registered, corresponding to the removal of coated/treated layers. The average volume loss was determined using surface profilometry from at least 3 tests taken at a specific sliding distance. The sliding distance travelled as a function of average volume loss was used to rank the different surface treatments investigated. This approach was more suitable to quantify relative improvements and evaluate the wear behaviour of these surface treatments than 'conventional' wear rates, due to the functionally-graded nature of coated TPT-layers giving a continually varying wear rate with depth.

### **3. Results and Discussion**

#### *3.1. Characterisation of PVD-TPT layers under investigation*

Knoop microhardness profiles obtained after TPT treatments shown in Table 1 are given in Fig.2. The Nitron treatment, which is currently used in aircraft landing gear bearings, provided the shallowest and least hard case among all treatments, as it is performed for a shorter time (120 mins) than all other nitriding and oxynitriding treatments. TPN-1 and TPN-2, nitriding treatments which were run for 240 mins, provided slightly harder and deeper case than Nitron. No differences in hardness profile can be seen between TPN-1 and TPN-2, although the latter had a final treatment hour at a higher bias voltage (-1000 V) in comparison to TPN-1 (-200 V). Finally, the best hardness profile is achieved by both oxynitriding treatments (TPON-1 and TPON-2), with a significant hardness increase in the first  $30 \mu\text{m}$  below the surface compared to any nitriding treatments. It is clear that the supply of oxygen for the first 60 minutes of treatment has a beneficial effect in terms of hardness profile. As with the nitriding treatments, the increase of bias voltage for the last 60 minutes in the oxynitriding treatment (TPON-2) did not promote any changes in hardness profile when compared to the low bias treatment (TPON-1).

Table 2 summarises some key properties of treated systems (TPT, PVD-coated and duplex) under investigation. Data for the parent Ti6Al4V alloy (i.e. uncoated and untreated) is also shown for comparison. Surface roughness values show that all TPT treatments (i.e., without PVD coating) promoted a small increase in surface roughness. The highest  $R_a$ -value ( $0.09 \mu\text{m}$ ) is achieved after the Nitron treatment, which is run at a high bias voltage ( $-1000 \text{ V}$ ) for 120 mins. For treatments carried out for 240 mins, it appears that those performed at a higher bias voltage ( $-1000 \text{ V}$ ) for the last 60 mins (e.g., TPN-2 and TPON-2) led to higher  $R_a$ -values, although the difference is statistically marginal. Conversely, PVD coating (see both TiN and CrAlN coatings on untreated Ti6Al4V) does not alter the surface finish of the parent Ti6Al4V alloy (i.e., untreated and uncoated). However,  $R_a$ -values for all duplex samples (i.e., TPT + PVD coating) were statistically similar to that of the parent Ti6Al4V alloy, indicating that a slight reduction in  $R_a$ -values occurred after coating. This can be attributed to the dense columnar coating morphology exhibited by both TiN and CrAlN coatings, which were grown at sufficient thickness to promote a reduction in surface roughness after TPT treatments. A fracture cross-section of CrAlN on TPON-2 is illustrated in Fig.3, showing that the CrAlN has a very dense columnar structure. It is worth noting that all coated/TPT layer systems under investigation had a significantly smaller  $R_a$ -value (about an order of magnitude) than the actual inner and outer bushes ( $R_a = 0.3\text{-}0.4\mu\text{m}$ ). Therefore, a combination of TPT + PVD coatings should not have a detrimental effect on surface roughness for aircraft bearing applications.

Coating thickness measured by ball cratering revealed that TiN-coated/treated samples were thicker than CrAlN-coated/treated samples. For a specific PVD coating, small variations in coating thickness ( $\sim 10\%$ ) occurred with different TPT treatments.

The Martens hardness obtained for TPT-treated samples (i.e., without coating) at a 10 mN load revealed that all treatments led to an increase in surface hardness compared to the uncoated, untreated parent material. At this load, the maximum penetration depth was  $\sim 0.160\text{-}0.170 \mu\text{m}$  and it was not possible to ascertain any differences between nitriding and oxynitriding treatments, as the Martens hardness values were statistically similar for all TPT samples. However, when the final load was decreased to 2 mN (corresponding to a maximum penetration depth of  $0.060\text{-}0.070 \mu\text{m}$ ), it became apparent that the treatments with the highest surface hardness were TPON-2 and TPN-2, i.e., the ones having the higher bias voltage ( $-1000 \text{ V}$ ) for the last 60 mins of treatment. It is worth noting that Nitron (run for 120 mins at  $-1000 \text{ V}$ ) also exhibited higher Martens hardness than TPN-1 and TPON-1 (both run at  $-200 \text{ V}$ ) but lower than those achieved by TPON-2 and TPN-2. Finally, when a 750 mN load was used and penetration depth was high, the highest Martens hardness values were recorded for both TPON-1 and TPON-2 samples. This can be attributed to a harder and deeper case provided by oxynitriding treatments, as detected by microhardness profile measurements. At this load, the hardness of the Nitron treatment is similar to that of the untreated Ti6Al4V alloy, whilst the other nitriding treatments (TPN-1 and TPN-2) still provide higher hardness values than the untreated parent material. These results indicate that the load-bearing capacity of TPT treatments decrease in the following order: triode plasma oxynitriding (TPON-1 and TPON-2), triode plasma nitriding (TPN-1 and TPN-2) and Nitron (surface hardening treatment currently applied to aircraft landing gear bearings).

For PVD-coated samples (PVD on untreated Ti6Al4V and PVD on TPT-treated Ti6Al4V), the Martens hardness values (HM) measured at a 10 mN load reflect the hardness of PVD coatings (TiN or CrAlN) without any contribution of the underlying substrate. At this load, the overall penetration was only  $\sim 5\text{-}7\%$  of the coating thickness so that the contribution of any underlying substrate to hardness values can be assumed to be negligible. Although HM values obtained for CrAlN on untreated and TPT-treated substrates were slightly higher than those for TiN on untreated and TPT-treated substrates, the standard deviations indicate that all coated or

coated/treated systems had statistically similar HM values, independent of coating type. At 750 mN, the contribution of the underlying substrate to HM values was considerable. For a specific PVD coating, higher HM values were obtained when the Ti6Al4V substrate was TPT-treated, suggesting that TPT layers improve the load-bearing capacity of coated Ti6Al4V. The only exception was TiN on Nitron, which displayed similar hardness to TiN on untreated Ti6Al4V alloy. This can possibly be attributed to variations in coating thickness, as Nitron-treated Ti6Al4V had a thinner TiN coating (2.5  $\mu\text{m}$ ) than untreated Ti6Al4V (2.8  $\mu\text{m}$ ) and the penetration depth at this much higher indentation load was 2.5  $\mu\text{m}$  for the former and 2.4  $\mu\text{m}$  for the latter.

GAXRD results are presented in Fig.4. Although differences between TPT treatments are subtle, it is possible to infer that titanium nitrides are formed at the surface of the Ti6Al4V alloy after all nitriding and oxynitriding treatments. For oxynitriding treatments, no titanium oxide phases were detected, indicating that a post-nitriding treatment for 180 mins after previous 60 mins of oxidation was effective in disrupting the oxide layer (mainly rutile) which is almost instantly formed at the sample surface after oxidation treatments. This is an important result in terms of subsequent PVD deposition onto TPT-treated surfaces, as it is well known that surface oxides usually compromise PVD coating/substrate adhesion.

Critical loads obtained from scratch adhesion tests are given in Fig.5. For a given type of PVD coating (i.e., TiN or CrAlN), higher critical loads were always recorded for duplex samples (TPT + PVD coating) than for PVD coating on untreated Ti6Al4V alloy, as hardened layers resulting from all TPT treatments improved the load support for TiN and CrAlN coatings.

For instance, TiN on untreated Ti6Al4V alloy failed adhesively at very low critical loads and did not exhibit any cohesive failures prior to adhesive ones (no  $L_{C1}$  was recorded). TiN on Nitron (current technology applied to aircraft landing gear bearings) showed higher critical loads than TiN on untreated Ti6Al4V but displayed lower adhesion than TiN on TPN-1 and TiN on TPN-2. As previously shown by microhardness profile and nanoindentation measurements, the load support for PVD coatings increased in the order Nitron < TPN-1 and TPN-2 < TPON-1 and TPON-2. Therefore, higher critical loads for TiN on TPN-1 and TiN on TPN-2 are expected than for TiN on Nitron. Nevertheless, the highest critical loads for TiN-coated samples were recorded when TiN was deposited onto TPN-2, the treatment run at a higher bias voltage (-1000 V) for the last 60 mins. This result cannot be explained by load support, as both TPN-1 and TPN-2 exhibited similar hardness profiles.

For CrAlN coatings, a similar trend to that described for TiN is also observed. Higher critical loads were recorded for CrAlN on all TPT treatments than for CrAlN on untreated Ti6Al4V alloy. Also, CrAlN on untreated parent material exhibited better adhesion than TiN on untreated Ti6Al4V, even though the former coating was significantly thinner than the latter. The highest critical loads were recorded for CrAlN on TPN-2 and CrAlN on TPON-2. The critical loads for these two duplex systems were comparable to those for TiN on TPN-2. If load support was the determining factor influencing coating/substrate adhesion (and therefore critical loads), one would expect CrAlN on TPON-1 to have yielded higher critical loads than CrAlN on TPN-2, as the former TPT treatment (oxynitriding) has a harder and deeper layer than the latter (nitriding). However, the highest critical loads were always exhibited by PVD coatings deposited onto TPT treatments run at a higher bias voltage (-1000 V) for the last hour of treatment (see TiN on TPN-2, CrAlN on TPN-2 and CrAlN on TPON-2). This may suggest that the last hour of treatment at a higher bias voltage improved coating/substrate adhesion. However, the reason for this improvement is not completely understood. A higher bias voltage (-1000 V) for the final hour of treatment translates in higher ion energies (especially at the low pressures used for nitriding and oxynitriding treatments carried out in this investigation), which could enhance the formation of titanium nitride at the sample surface when compared to treatments performed at

low bias voltages (-200 V). It is worth noting that this final hour of treatment corresponds to a small fraction (25%) of the total treatment time. Therefore, the effect of bias voltage on TPT treatments is expected to be small. Although GAXRD analyses did not indicate any significant differences between TPN-1 and TPN-2 or TPON-1 and TPON-2 in terms of titanium nitride formation, nanoindentation results at a final load of 2 mN indicated that treatments (either nitriding or oxynitriding) carried out at a higher bias voltage for the last hour of treatment led to harder surfaces than their low voltage counterparts. Surface roughness is another parameter that could have influenced scratch test results. However, surface roughness measurements (Table 2) revealed that after PVD coating (either TiN or CrAlN), all TPT-PVD coating combinations (duplex samples) exhibited small, similar  $R_a$  values independent of whether or not a high bias voltage had been used during the last hour of TPT treatments.

### 3.2. FEA of bush tests

Fig.6 shows a plot of the normal stress  $S_y$  relative to the global axis (and the defined path shown in the bush assembly) as a result of a 50 kN load. Although the FEA makes no allowance for the bending of the shaft, it suggests that there is an edge affect due to the bush clearance. Fig.6 shows that the resulting stress distribution in a path parallel to the shaft axis peaks near both edges of the bush assembly. The central portion of the bush (about 80% of the total distance along the path shown in Fig.6) has a pressure of ~ 150 MPa, which is 50% greater than the pressure calculated from projected area analysis (100 MPa for a test load of 50 kN). However, the pressure increases from the central portion of the bush assembly towards the edges until a value of 229 MPa is attained, which is approximately 225% greater than the pressure calculated from projected area analysis. Therefore, FEA analysis of the bush test assembly indicates that peak pressures are expected to occur near both edges during the test; these peak pressures have a magnitude of at least ~ 2.25 times the pressure calculated from the projected area analysis. Although further results are not shown in this paper, FEA analysis carried out at higher test loads (80 and 100 kN) indicated similar trends for the stress distribution in the bush assembly.

### 3.3. Bush tests

Bush test results are shown in Table 3. The test successfully discriminated relative improvements provided by each surface treatment and enabled coated/treated layers to be ranked accordingly. Among all surface treatment combinations, CrAlN on TPN-2 and CrAlN on TPON-2 were the only ones able to withstand test loads up to 60 kN (corresponding to a peak pressure of 270 MPa) without failing. Bush test results also show that a duplex combination of PVD coating on TPT layer significantly outperforms PVD-coated bushes without TPT layers. Bush tests indicate that combinations of CrAlN on either TPN-2 or TPON-2 plasma treatments have immense potential to be applied on a diverse range of lightweight metal-to-metal bearings and are promising surface treatments to extend the current bearing pressures up to (and beyond) the desired 220 MPa level. Finally, the inspection of failed bush pairs after testing corroborates the stress distribution obtained by FEA (Fig.6), with both outer and inner bushes failing near the edges where the maximum peak pressure is expected to occur in the bush assembly. An example of a bush pair that failed after testing is shown in Fig.7.

### 3.4. Reciprocating sliding wear tests

Reciprocating sliding wear results are given in Figs.8a-c. Independent of the test condition, it is clearly seen that combinations of PVD coating + TPT layers or solely PVD coatings improve the wear behaviour of the uncoated, untreated Ti6Al4V alloy.

For tests carried out at a load of 4 N using a WC-Co ball (Fig.8a), results show that TiN on all plasma treated Ti6Al4V alloy outperformed TiN on untreated Ti6Al4V alloy. The best

combination was TiN on TPN-1, which displayed negligible volume loss at a sliding distance of 1,000 m and still the smallest average volume loss at a sliding distance of 1,500 m. When the test load was increased to 13.5 N (Fig.8b), similar trends were observed, with TiN on TPN-1 exhibiting the best wear performance, followed by TiN on TPN-2 and TiN on Nitron. However, all samples failed at considerably shorter distances under the higher load.

For tests carried out at a load of 13.5 N using a sapphire ball (Fig.8c), results also show that CrAlN on all plasma treated Ti6Al4V alloy outperformed CrAlN on untreated Ti6Al4V alloy. At this higher load, CrAlN lasts much longer distances than TiN, even though the former coating was tested with a (more aggressive) sapphire ball. The best performance is achieved by CrAlN on TPON-2, followed by CrAlN on TPN-2. The CrAlN on TPON-2 and CrAlN on TPN-2 both showed negligible volume loss up to sliding distances of 2,750 m and 2,500 m respectively. It is also worth noting that CrAlN, although significantly thinner than TiN, exhibited an overall superior performance to TiN in reciprocating sliding wear tests. Results obtained from reciprocating sliding wear tests correlate closely in ranking order to the bush test results, with both tests indicating that CrAlN on either TPON-2-treated or TPN-2-treated Ti6Al4V alloy outperformed all other systems under investigation.

#### **4. Conclusions**

Bush test and reciprocating sliding wear results indicate that CrAlN on Ti6Al4V treated with TPON-2 or TPN-2 are the best PVD coating-TPT combinations for aircraft bearing applications. FEA of bush tests also demonstrated that (at test loads of 60 kN) peak pressures of 270 MPa are achievable without failure, suggesting that both CrAlN on TPON-2 and CrAlN on TPN-2 should be able to withstand such pressures in bearing applications. These two treatments have great potential to extend the current lightweight bearing pressures in aircraft up to (and beyond) 220 MPa and be applied to full size bearings for simulated aircraft-lifetime tests.

#### **Acknowledgements**

The authors are greatly indebted to the UK DTI/TSB for financial support under their Collaborative Research & Development Projects, Project No TP 22076, LIB-TEC.

#### **References**

- [1] P. Smith, US Patent No 7165890, 23 Jan. 2007.
- [2] B.R. Lanning, R. Wei, Surf. Coat. Technol. 186 (2004) 314-319.
- [3] S. Ma, K. Xu, W. Jie, Surf. Coat. Technol. 185 (2004) 205-209.
- [4] R. Wei, T. Booker, C. Rincon, J. Arps, Surf. Coat. Technol. 186 (2004) 305-313.
- [5] O. Kessler, H. Surm, F. Hoffmann, P. Mayr, Surf. Eng. 18 (2002) 299-304.
- [6] P.A. Dearnley, K.L. Dahm, H. Çimenoglu, Wear 256 (2004) 469-479.
- [7] H. Dong, W. Shi, T. Bell, Wear 225-229 (1999) 146-153.
- [8] H. Dong, T. Bell, Wear 238 (2000) 131-137.
- [9] H. Dong, X.Y. Li, Mater. Sci. Eng. A280 (2000) 303-310.
- [10] J.C. Avelar-Batista, E. Spain, J. Housden, A. Matthews, G.G. Fuentes, Surf. Coat. Technol. 200 (2005) 1954-1961.

## Tables

Table 1: TPT process conditions

TPT process	Pressure (Pa)	Gas composition	Time (mins)	Workpiece bias (V)
Nitron	2.0	20% Ar + 80% N <sub>2</sub>	120	-1000
TPN-1	0.4	30% Ar + 70% N <sub>2</sub>	240	-200
TPN-2	0.4	30% Ar + 70% N <sub>2</sub>	240	-200 (first 180 mins) -1000 (last 60 mins)
TPON-1	0.4	30% Ar + 70% O <sub>2</sub> (first 60 mins) 30% Ar + 70% N <sub>2</sub> (last 180 mins)	240	-200
TPON-2	0.4	30% Ar + 70% O <sub>2</sub> (first 60 mins) 30% Ar + 70% N <sub>2</sub> (last 180 mins)	240	-200 (first 180 mins) -1000 (last 60 mins)

Table 2: Surface roughness, TPT depth, coating thickness and Martens hardness of uncoated, untreated Ti6Al4V alloy and coated/treated layers.

Surface treated systems	Surface roughness, $R_a$ ( $\mu\text{m}$ )	Treatment thickness ( $\mu\text{m}$ )		Martens harness, HM (GPa)		
		TPT-layer	PVD coating	2 mN	10 mN	750 mN
Uncoated, untreated Ti6Al4V	0.04 $\pm$ 0.01	-----	-----	-----	3.5 $\pm$ 0.1	3.2 $\pm$ 0.1
Nitron	0.09 $\pm$ 0.01	15-20	-----	7.7 $\pm$ 0.4	7.3 $\pm$ 0.4	3.1 $\pm$ 0.1
TPN-1	0.06 $\pm$ 0.01	25-30	-----	7.0 $\pm$ 0.3	7.5 $\pm$ 0.3	3.6 $\pm$ 0.1
TPN-2	0.07 $\pm$ 0.01	25-30	-----	8.0 $\pm$ 0.5	7.5 $\pm$ 0.4	3.4 $\pm$ 0.2
TPON-1	0.05 $\pm$ 0.01	35-40	-----	7.2 $\pm$ 0.2	7.5 $\pm$ 0.3	4.5 $\pm$ 0.1
TPON-2	0.07 $\pm$ 0.01	35-40	-----	9.2 $\pm$ 0.3	7.6 $\pm$ 0.4	4.6 $\pm$ 0.2
TiN on untreated Ti6Al4V	0.03 $\pm$ 0.01	-----	2.8 $\pm$ 0.2	-----	13 $\pm$ 2	4.4 $\pm$ 0.1
CrAlN on untreated Ti6Al4V	0.02 $\pm$ 0.01	-----	1.9 $\pm$ 0.1	-----	14 $\pm$ 1	3.3 $\pm$ 0.1
TiN on Nitron	0.05 $\pm$ 0.01	15-20	2.5 $\pm$ 0.1	-----	9 $\pm$ 2	4.3 $\pm$ 0.3
TiN on TPN-1-treated Ti6Al4V	0.05 $\pm$ 0.01	25-30	3.2 $\pm$ 0.2	-----	13 $\pm$ 3	5.0 $\pm$ 0.3
TiN on TPN-2-treated Ti6Al4V	0.05 $\pm$ 0.01	25-30	2.9 $\pm$ 0.2	-----	12 $\pm$ 2	5.1 $\pm$ 0.2
CrAlN on TPN-2-treated Ti6Al4V	0.05 $\pm$ 0.01	25-30	2.3 $\pm$ 0.1	-----	14 $\pm$ 3	4.7 $\pm$ 0.3
CrAlN on TPON-1-treated Ti6Al4V	0.05 $\pm$ 0.01	35-40	1.9 $\pm$ 0.1	-----	15 $\pm$ 2	5.4 $\pm$ 0.3
CrAlN on TPON-2-treated Ti6Al4V	0.06 $\pm$ 0.01	35-40	2.2 $\pm$ 0.1	-----	14 $\pm$ 1	5.2 $\pm$ 0.4

Table 3: Bush test results. A Pass mark at a certain load was given to coated/treated bush assemblies that did not fail up to 6,000 cycles in the test.

Bush specimens Load (kN) / Peak pressure (MPa) <sup>a</sup>	TiN- untreated Ti6Al4V	CrAlN- untreated Ti6Al4V	TiN- Nitron	TiN- TPN-1	CrAlN- TPN-2	CrAlN- TPON-1	CrAlN- TPON-2
10 / 45	<b>Pass</b>	-----	<b>Pass</b>	-----	-----	-----	-----
15 / 67.5	Fail	Fail	Fail	<b>Pass</b>	-----	-----	-----
20 / 90	Fail	-----	Fail	<b>Pass</b>	-----	-----	-----
25 / 112.5	-----	Fail	-----	Fail	-----	-----	-----
30 / 135	-----	-----	-----	Fail	-----	-----	-----
35 / 157.5	-----	-----	-----	-----	<b>Pass</b>	<b>Pass</b>	<b>Pass</b>
40 / 180	-----	-----	-----	-----	<b>Pass</b>	Fail	<b>Pass</b>
45 / 202.5	-----	-----	-----	-----	<b>Pass</b>		<b>Pass</b>
50 / 225	-----	-----	-----	-----	<b>Pass</b>		<b>Pass</b>
55 / 247.5	-----	-----	-----	-----	<b>Pass</b>		<b>Pass</b>
60 / 270	-----	-----	-----	-----	<b>Pass</b>		<b>Pass</b>

<sup>a</sup> Peak pressures were obtained from FEA results on bush assembly.

## Figure Captions

Fig.1: Schematic of bush test assembly, showing interfaces 1, 2 and 3 where surface to node contact was defined for FEA.

Fig.2: Knoop microhardness profile of TPT-treated Ti6Al4V samples.

Fig. 3: SEM fracture cross-section of a 2.2  $\mu\text{m}$  thick CrAlN coating deposited on TPON-2-treated Ti6Al4V. The CrAlN coating exhibits a very dense columnar structure.

Fig.4: GAXRD results for TPT-treated samples (i.e., without PVD coating). Data for parent material (untreated Ti6Al4V) is also shown for comparison. The diffractograms were shifted vertically for clarity purposes.

Fig.5: Scratch adhesion test results for PVD coatings on untreated Ti6Al4V alloy and duplex samples (TPT-treated Ti6Al4V alloy + PVD coatings).

Fig.6: Plot of the normal stress  $S_y$  relative to the global axis (and defined path shown in bush assembly) as a result of a 50 kN load. The path was taken parallel to the shaft axis.

Fig.7: Bush pair treated with TPN-1 and coated with CrAlN that failed after testing. The outer and inner bushes failed near the edges where maximum peak stresses are expected to occur according to FEA.

Fig.8: Plots of average wear loss versus sliding distance travelled for investigated samples under a 4 N test load and 10 mm WC-Co ball (a), 13.5 N test load and 10 mm WC-Co ball (b) and 13.5 N test load and 10 mm sapphire ball (c).

**Figures**

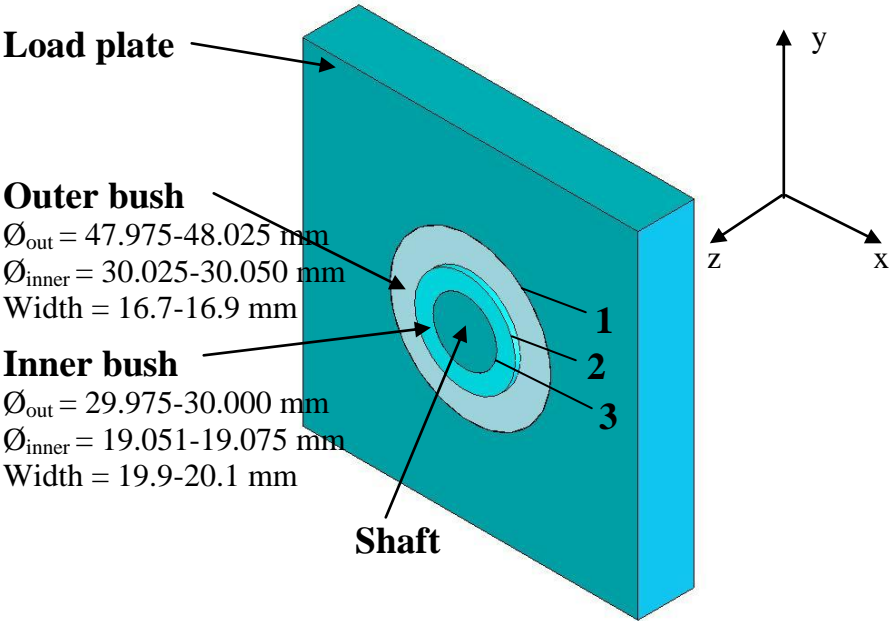


Fig.1

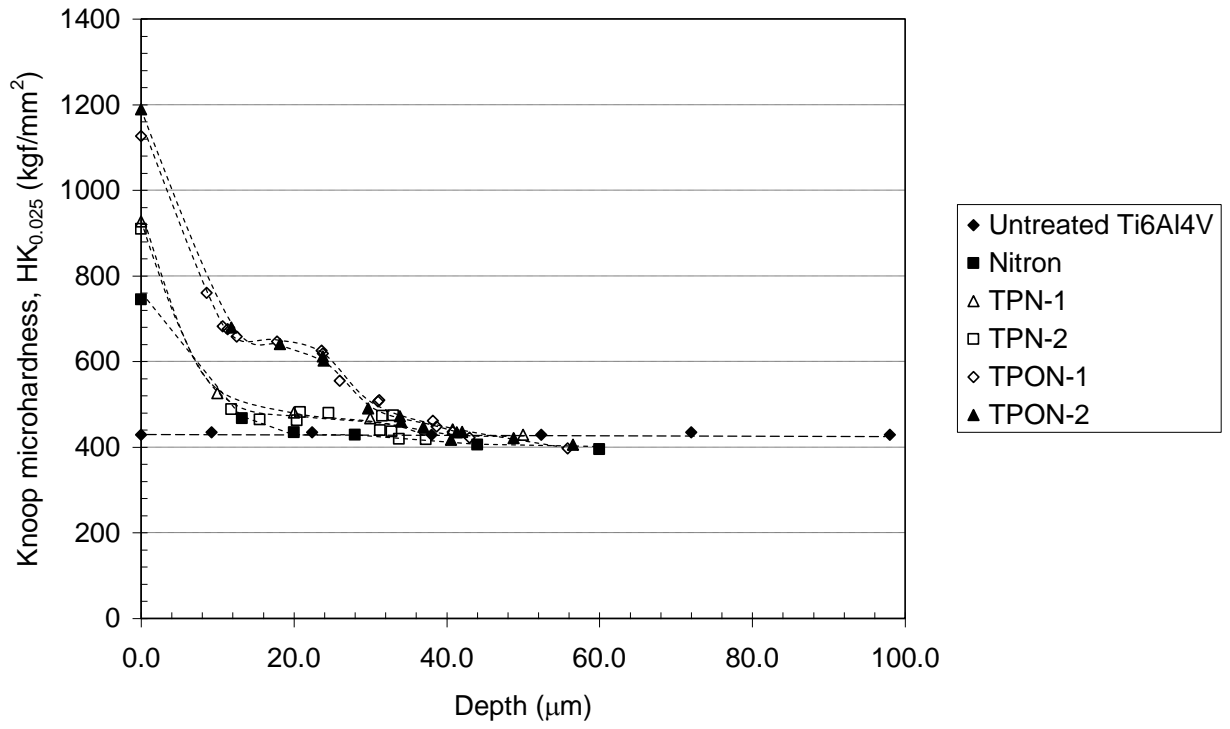


Fig.2

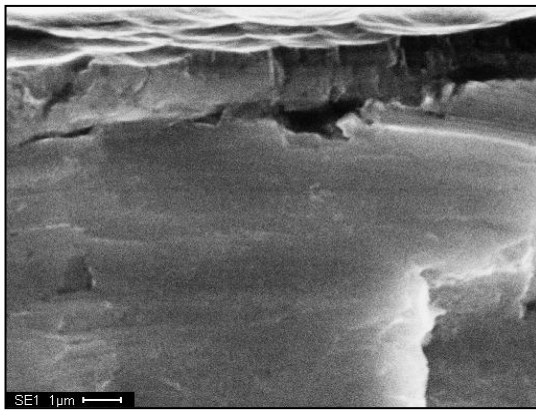


Fig.3

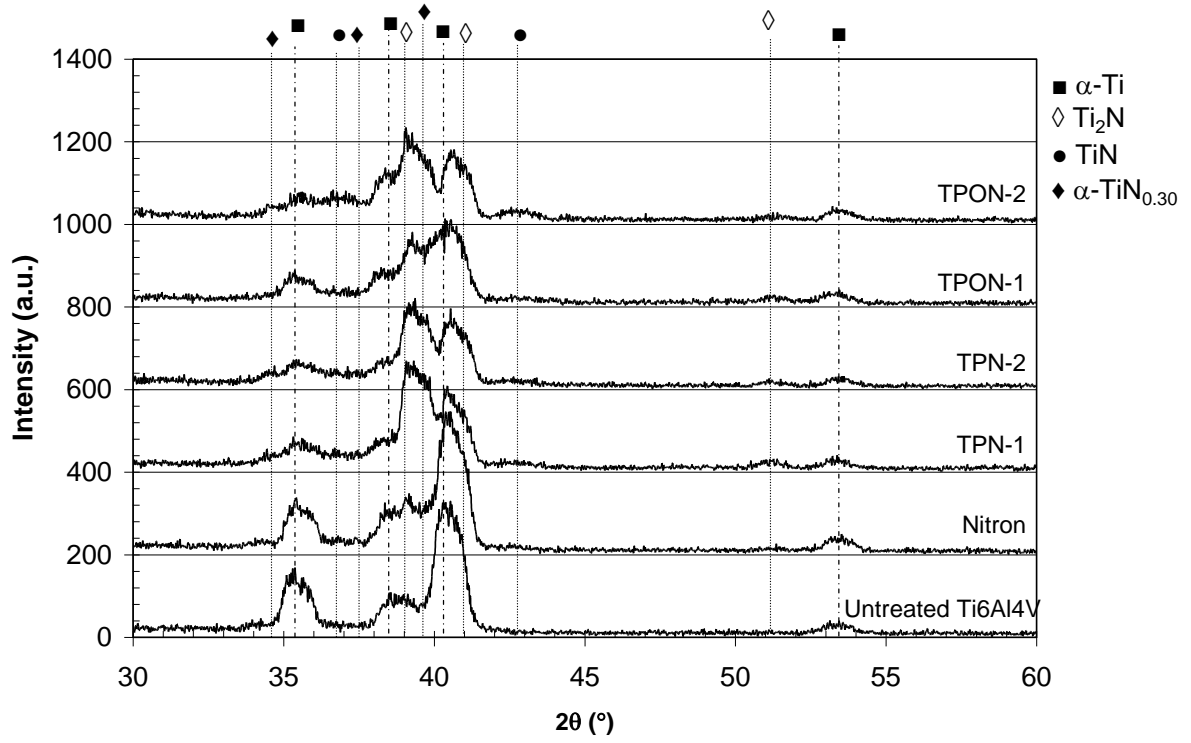


Fig.4

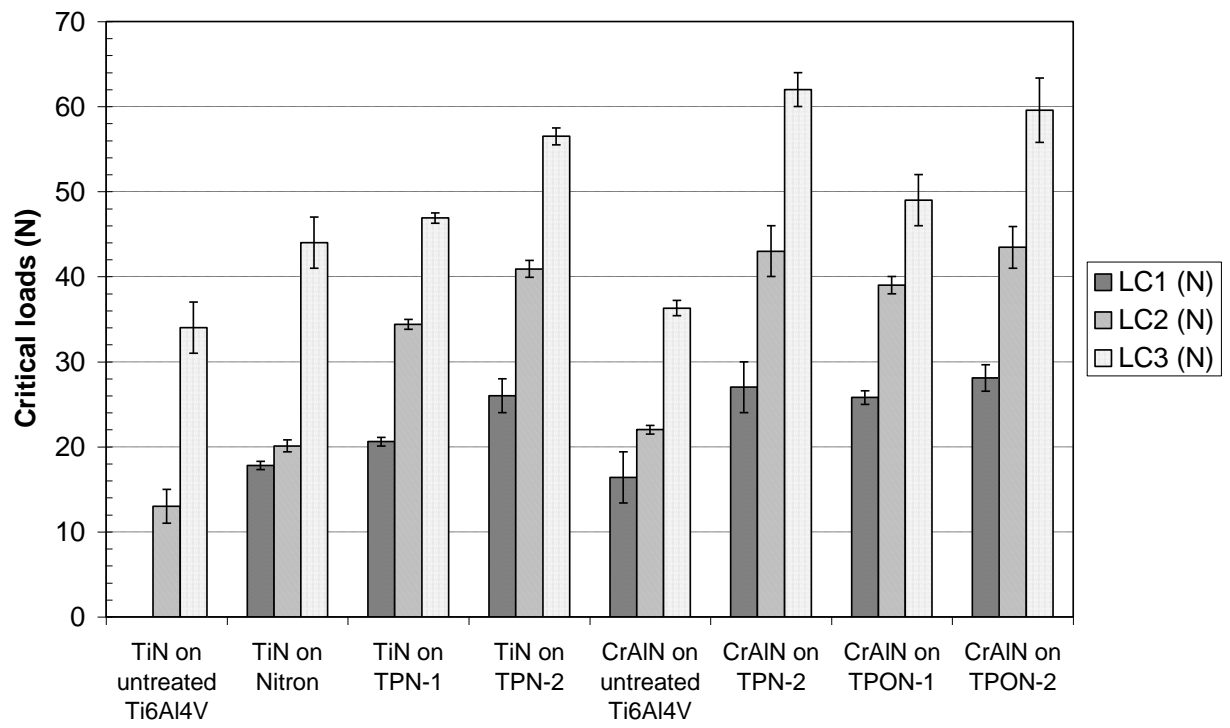


Fig.5

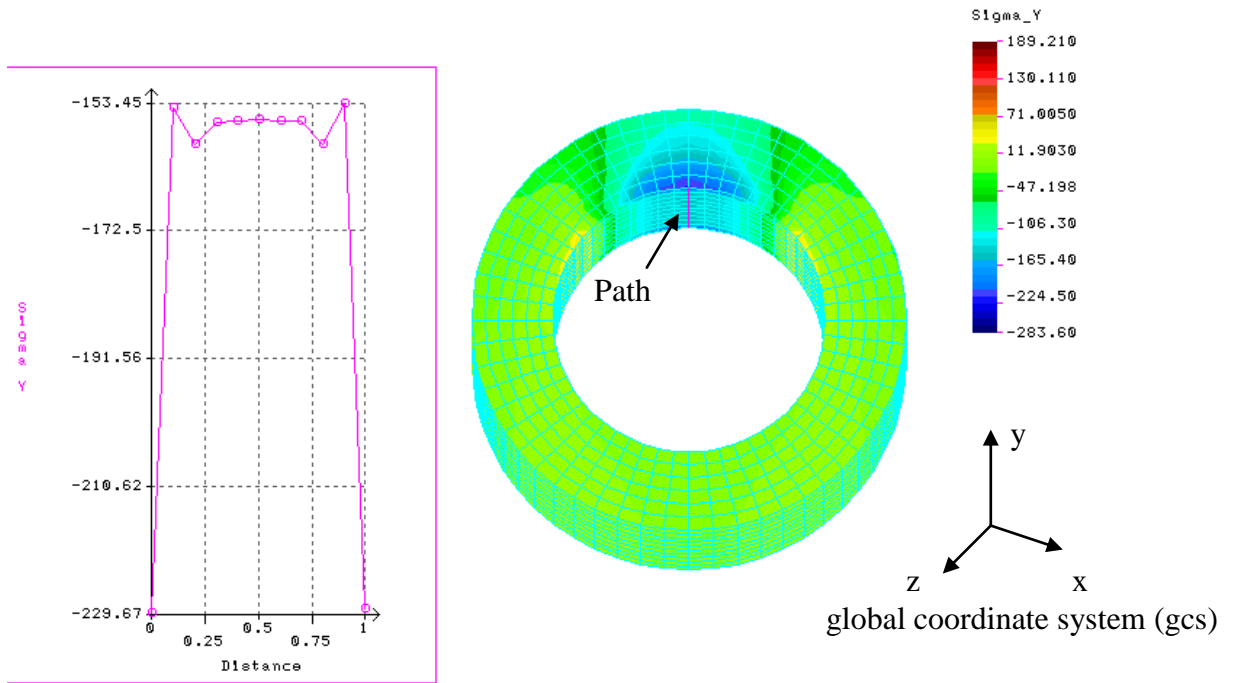


Fig.6

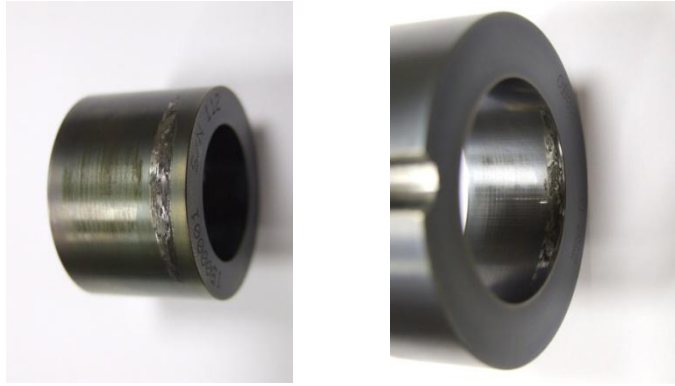


Fig.7

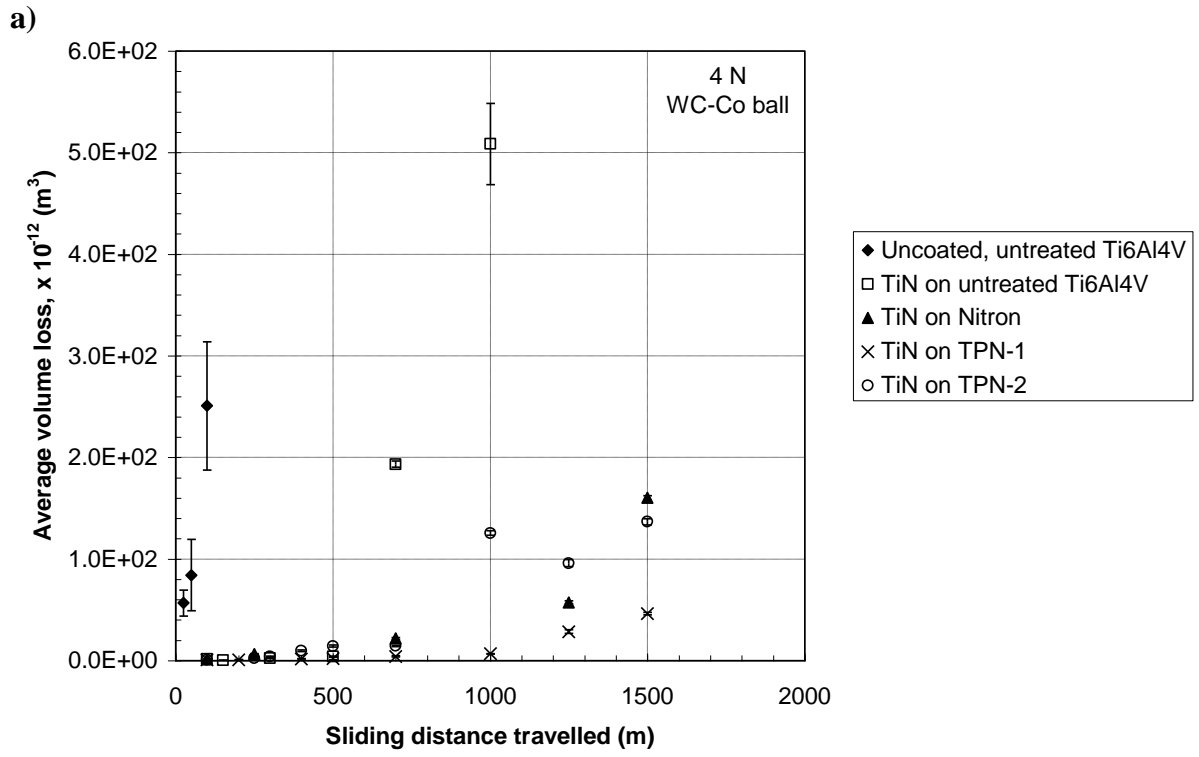


Fig.8a

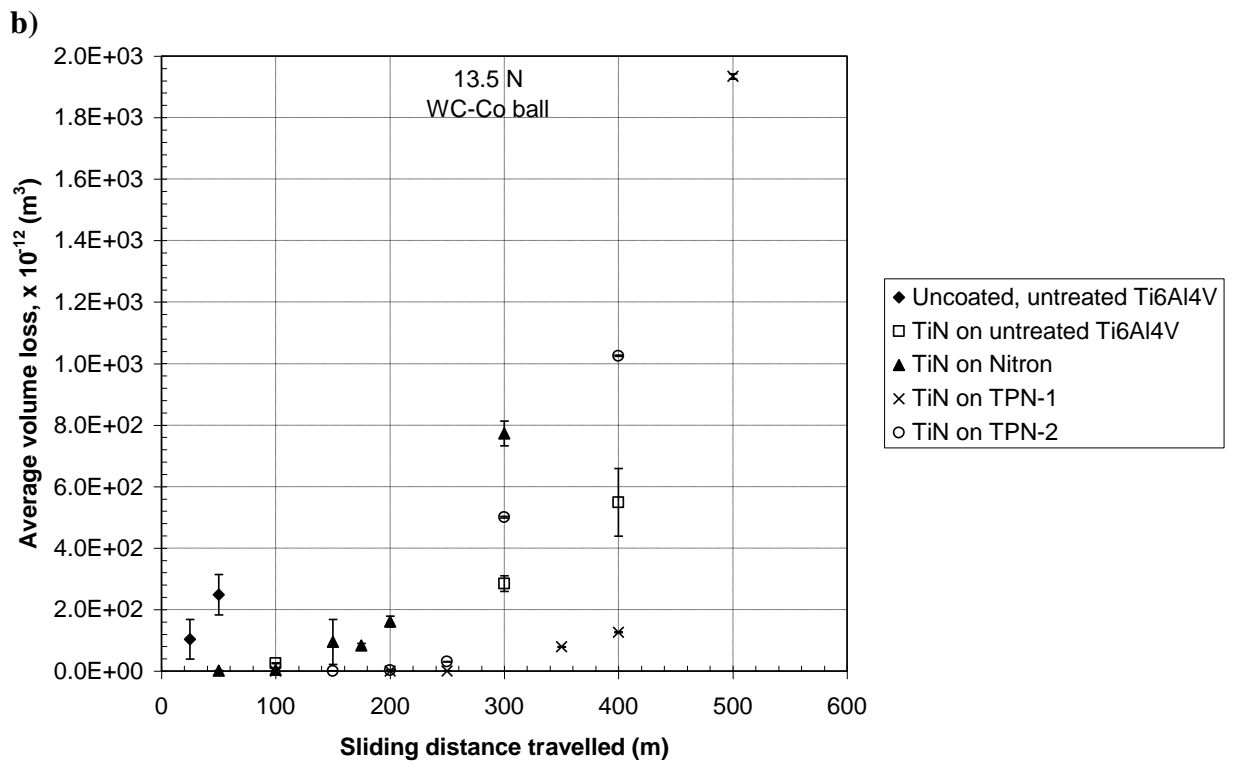


Fig.8b

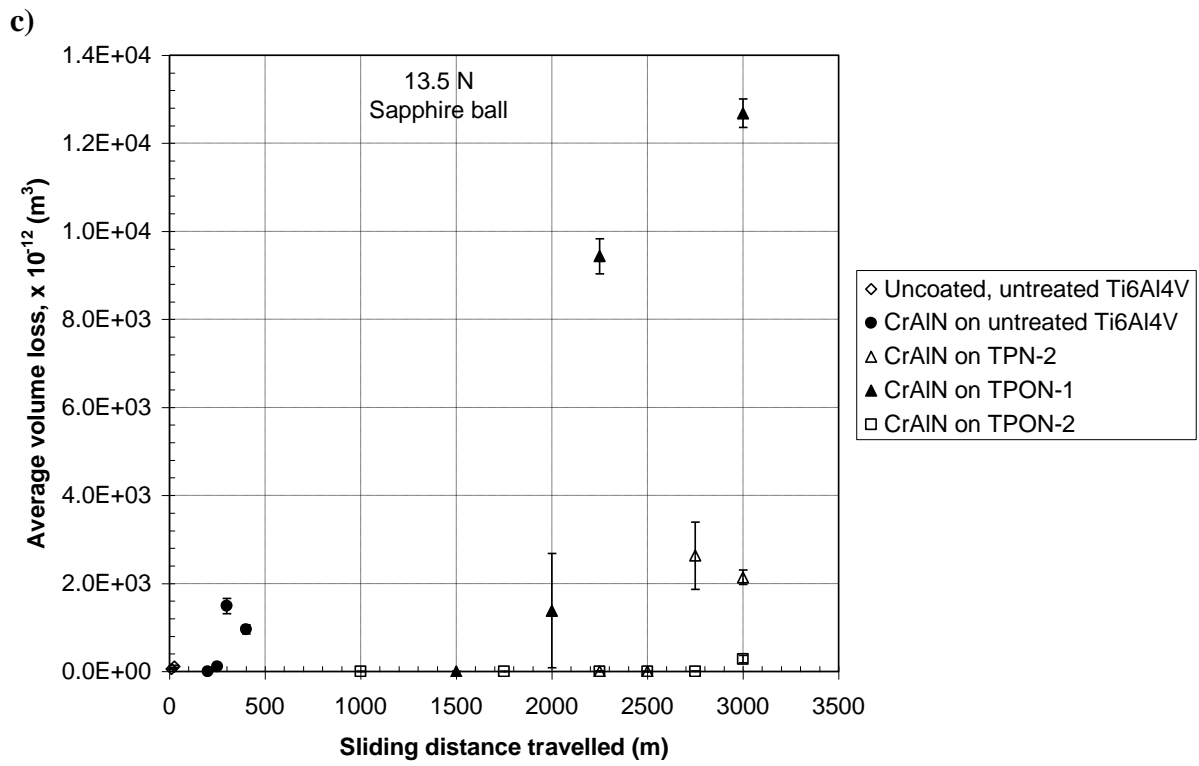


Fig. 8c